Electronic Supplementary Material (ESI) for ChemComm.

Supplementary material for manuscript:

Synthesis, X-ray characterization and regium bonding interactions of a trichloro(1-hexylcytosine)-gold(III) complex

Angel Terrón,[a,*] Jordi Buils,[a] Tiddo J. Mooibroek,[b,*] Miquel Barceló-Oliver,[a] Angel García-Raso, Juan J. Fiol and Antonio Frontera[a,*]

Table of contents:

Overview of known purine and pyrimidine(-like) Au(III) X-ray structures	**Pag 2**
Materials and methods	**Pag 3**
Single Crystal X-ray Diffraction (SC-XRD)	**Pag 4**
Theoretical methods	**Pag 6**
Details of the Cambridge Structure Database analysis	**Pag 7**
References	**Pag 13**

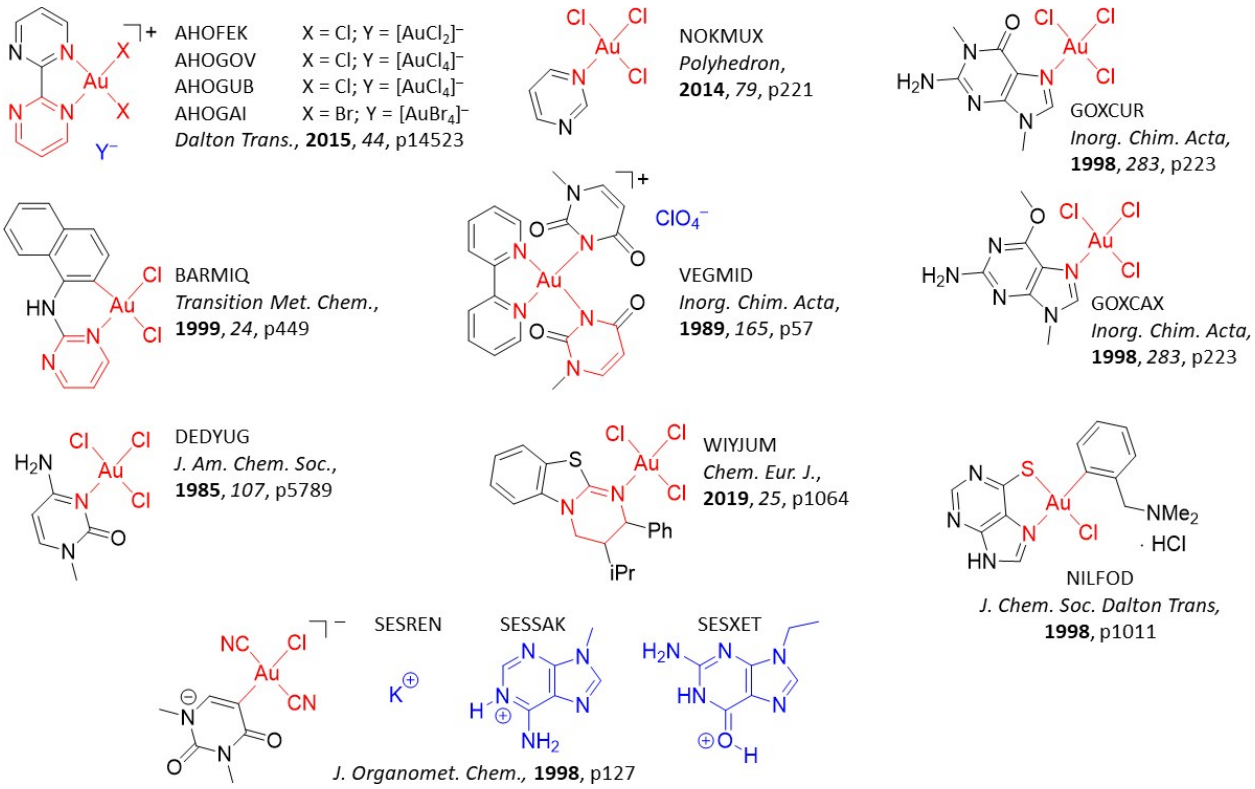

Figure S1. Overview of all twelve purine or pyrimidine(-like) X-ray structures currently present within the Cambridge Structure Database.

Materials and methods

All chemicals were obtained from commercial sources (Sigma-Aldrich) and used without further purification. N^1-hexylcytosine was obtained as previously published.[1]

Elemental analysis of C, H and N was carried out using a Carlo-Erba (1106 and 1108) and Microanalyzer Thermo Finnigan Flash 1112 apparatus.

The FT-IR spectra in the solid state (KBr pellets) were recorded in the 4000-400 cm^{-1} range on a Bruker Tensor 27 spectrometer.

The ^1H NMR spectra were recorded at room temperature on a Bruker AMX 300 (300 MHz). Proton chemical shifts in DMSO-d_6 were referenced itself to the residual peak from the solvent DMSO-d_6 [^1H NMR d = 2.50 ppm].

For the ESI-HRMS, an Orbitrap mass spectrometer (ThermoFisher Scientific) operating with a heated electrospray interface (HESI) was employed and the spectra was recorded in negative mode. The temperature of ion transfer capillary was set to 320 °C, the spray voltage was set to 2.9 kV in negative mode and S-lens RF level 50 AU. Direct injection in Full scan acquisition mode over a range of 190-1000 m/z was performed with a resolution of 140000.

Synthesis of [$AuCl_3$(N^1-hexylcytosine,*N(3)*)], chemical formula $C_{10}H_{17}AuCl_3N_3O$

To a solution of 0.5 mmol $Na[AuCl_4]\cdot 2H_2O$ in 20 ml of water quality Milli-Q, 0.5 mmol of N^1-heylcytosine were added as a dispersion. The mixture in the absence of light was stirred for 4 days. A yellow precipitated appeared, the solid was filtered off and recrystallized in a mixture of acetonitrile (10ml) and water (0.1ml). After two days, yellow needles appeared mixed with white crystals of the ligand. The selected crystals were adequate for a monocrystal X-ray study.

The molecular unity was identified by ESI-HRMS with a good and coherent isotopical distribution. To obtain the compound with better yield and without impurities of the ligand, a different synthetic procedure was designed.

Two solutions, one containing of 0.5 mmol of $Na[AuCl_4]\cdot 2H_2O$ solved in 2 ml of water Milli-Q and other of 0.5 mmol of N^1-hexylcytosine in 20 ml of dioxane , were mixed. The mixture was stirred for 24 hours in the absence of light. A final yellow solution is obtained. The solution was rota-evaporated to a few millilitres and dried in a desiccator. The yellow solid obtained was powdered down and cleaned with chloroform stirring for 24 hours. The yellow solid was filtered off and dried, the yield was 49%.

Elemental analysis of $[AuCl_3(C_{10}H_{17}N_3O)]_2\cdot 3(CHCl_3)$: Experimental: C, 20.15 %, H, 2.75 % and N, 6.58 %; Calculated for $C_{23}H_{37}Au_2Cl_{15}N_6O_2$: C, 20.38 %, H, 2.75 % and N, 6.20 %.

ESI-HRMS: Exact mass (m/z), 496.0032 (M-H); Calculated for $C_{10}H_{16}ON_3{}^{197}Au^{35}Cl_3$, 496.0030.

IR(cm^{-1}): 3419.91 vs; 3328.60 vs; 3222.82 s; 3114.86w; 3073.83 w; 2956.23 m; 2924.91 m; 2854.20 m; 1721.86 w; 1671.57 vs; 1640.29 vs; 1620.84 vs; 1530.08 m ; 1510.79 vs; 1462.04 m; 1398.33 s; 1381.30 s.

^1H-NMR: The complex dissolves with decomposition in DMSO giving free ligand and a set of resonances that are consistent with coodinated ligand (presumably complex **1**). These signals were: ***δ*** (ppm) 9.40 (s(br), 1H, H(4a)), 9.12 (s(br), 1H, H(4b)), 7.90 (d, 1H, H(6), *J* = 7.50Hz), 6.00 (d, 1H, H(5), *J* = 6.30Hz), 3.78 (t, 2H, H(7), *J* = 7.20 Hz), 1.54 (m(br), 2H, H(8)), 1.25 (s(br), 6H, H(9,10,11)), 0.85 (t, 3H, H(12), *J* = 6.30 Hz).

The neutral complex is not soluble in water and chloroform, but soluble in other organic solvents like acetonitrile or 1,4-dioxane.

Single Crystal X-ray Diffraction (SC-XRD)

Suitable crystals of **[$AuCl_3$(N^1-hexylcytosine,*N(3)*)]** were selected for X-ray single crystal diffraction experiments, covered with oil (Infineum V8512, formerly known as Paratone N) and mounted at the tip of a nylon CryoLoop on a BRUKER-NONIUS X8 APEX-II KAPPA CCD diffractometer using graphite monochromated MoKα radiation (λ = 0.7107 Å). Crystallographic data were collected at 300(2) K. Data were corrected for Lorentz and polarisation effects and for absorption by SADABS.[2] The structural resolution procedure was made using the WinGX package.[3] Solving for structure factor phases was performed by SHELXT-2014.[4] For the full matrix refinement SHELXL-2017/1[19,5] was used. The structures were checked for higher symmetry with help of the program PLATON.[6] H-atoms were introduced in calculated positions and refined riding on their parent atoms. A summary of refinement parameters can also be seen in Table S1. Also, in Table S2 the bond lengths, angles and torsion angles for the coordination environment to gold(III) is described. The intermolecular distance and angles for the hydrogen bonds found within structure 1 are summarized in Table S3.

Table S1. Crystal data and structure refinement for [$AuCl_3$(N^1-hexylcytosine,N(3)].

Empirical formula		s
Formula weight		498.58
Temperature (K)		300(2)
Wavelength (Å)		0.71073
Crystal system		Monoclinic
Space group		P 21/c
Unit cell dimensions	a (Å)	7.0041(19)
	b (Å)	15.654(4)
	c (Å)	16.326(4)
	β (°)	115.405(8)
Volume ($Å^3$)		1617.0(7)
Z		4
Density (calculated) (Mg/m^3)		2.048
Absorption coefficient (mm^{-1})		9.586
F(000)		944
Crystal size (mm^3)		0.200 x 0.070 x 0.070
Theta range for data collection (°)		1.897 to 28.508
Index ranges		-9 <= h <= 9
		0 <= k <= 20
		-21 <= l <= 21
Reflections collected		7301
Independent reflections		3861 [R(int) = 0.0687]
Completeness to theta = 25.242 ° (%)		100.0
Absorption correction		Semi-empirical from equivalents
Max. and min. transmission		1 and 0.628
Refinement method		Full-matrix least-squares on F2
Data / restraints / parameters		3861 / 46 / 164
Goodness-of-fit on F2		0.880
Final R indices [I>2sigma(I)]	R1	0.0516
	wR2	0.0975
R indices (all data)	R1	0.1145
	wR2	0.1136
Largest diff. peak and hole ($e \cdot Å^{-3}$)		0.969 and -1.958

Table S2. Coordination environament bond lengths and angles for **[$AuCl_3$(N^1-hexylcytosine,N(3)].**

distances (Å)		angles (°)		torsions (°)	
Au(1)-N(3)	2.021(8)	N(3)-Au(1)-Cl(2)	176.1(2)	Cl(1)-Au(1)-N(3)-C(2)	76.4(8)
Au(1)-Cl(2)	2.256(3)	N(3)-Au(1)-Cl(3)	88.6(2)	Cl(1)-Au(1)-N(3)-C(4)	-106.6(8)
Au(1)-Cl(3)	2.257(3)	Cl(2)-Au(1)-Cl(3)	91.09(12)	Cl(2)-Au(1)-N(3)-C(2)	-19(4)
Au(1)-Cl(1)	2.287(3)	N(3)-Au(1)-Cl(1)	90.0(2)	Cl(2)-Au(1)-N(3)-C(4)	159(3)
		Cl(2)-Au(1)-Cl(1)	90.39(11)	Cl(3)-Au(1)-N(3)-C(2)	-104.5(7)
		Cl(3)-Au(1)-Cl(1)	178.34(10)	Cl(3)-Au(1)-N(3)-C(4)	72.6(8)

Table S3. Distances and angles for the hydrogen bond interactions in **[$AuCl_3$(N^1-hexylcytosine,N(3)].**

D-H···A	d(D-H) (Å)	d(H···A) (Å)	d(D···A) (Å)	<(DHA) (°)
N(4)-H(4A)···Cl(1)#1	0.86	2.66	3.451(10)	153.2
N(4)-H(4B)···Cl(1)#2	0.86	2.71	3.472(8)	149.0
C(5)-H(5)···O(2)#2	0.93	2.33	3.166(11)	148.7
C(6)-H(6)···Cl(2)#3	0.93	2.95	3.790(13)	150.8
C(7)-H(7B)···Cl(3)#4	0.97	2.89	3.684(11)	139.4
C(7)-H(7A)···Cl(2)#3	0.97	2.88	3.797(12)	158.4

Symmetry transformations used to generate equivalent atoms:
#1: -x+1,-y+1,-z+1; #2: x-1,y,z; #3: x,-y+3/2,z+1/2; #4: x+1,-y+3/2,z+1/2

Theoretical methods

The energies of the complexes included in this study were computed at the PBE1PBE -D3/def2-TZVP level of theory by using the program Gaussian-16.[7] The interaction energy (or binding energy in this work) ΔE, is defined as the energy difference between the dimer complex and the sum of the energies of the monomers. For the calculations we have used the Weigend def2-TZVP[8,9] basis set and the PBE1PBE DFT functional.[10] The MEP (Molecular Electrostatic Potential) surfaces calculations have been computed using Gaussian-16 software at the PBE1PBE-D3/def2-TZVP level of theory. The AIM formalism elucidated bond paths via analysis of the topology of the electron density,[11,12] using the PBE1PBE-D3/def2-TZVP wavefuntion and making use of the AIMALL program.[13]

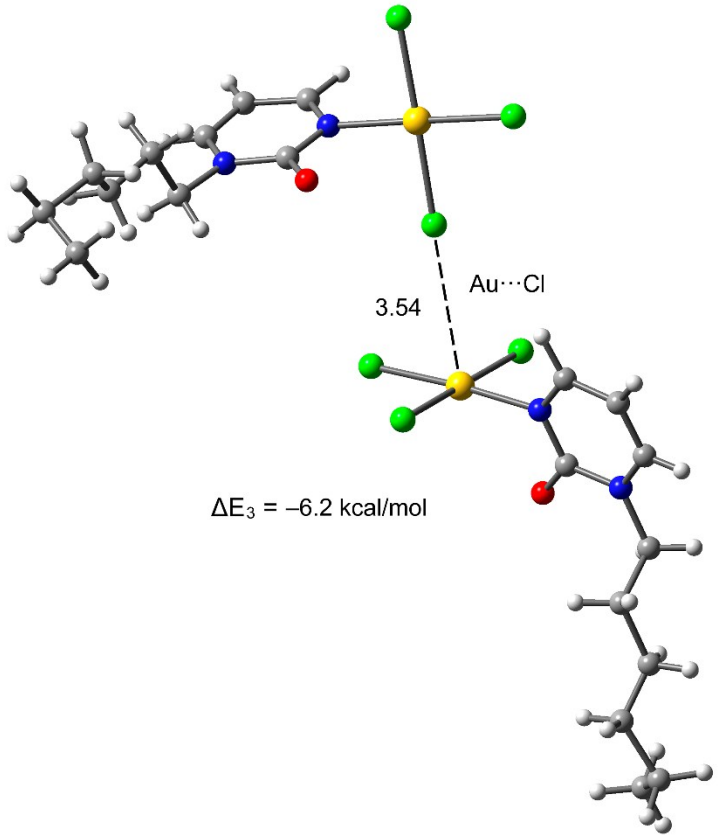

Figure S2. Structure (PBE0-D3/def2-TZVP) of an alternative arrangement of a dimeric structure of **1** (without the amine, see also Figure 4, right) held together with only one regium bonding interaction; one complex was forced to rotate 90° around one intermolecular Cl···Au bond to give a single Au–Cl···Au angle near 180° (geometry optimization led to the original dimer). The interaction energy (ΔE_3) of –6.2 kcal/mol is less then halve the stabilization energy of a dimer with two Cl···Au interactions (ΔE_2 = –15.9; Figure 4, right). This might be due to the diminished electron density at the extension of the Au – Cl bonds, as can also be seen in Figure 3. Alternatively, or concomitantly, the extra stabilization energy of ΔE_2 might be due to a synergistic effect because both monomers can act as an electron donor with a Cl-atom as well as an electron acceptor with their Au atoms.

CSD search

The Cambridge Structure Database (CSD) version 5.41 with updates until November 2019 was inspected using ConQuest version 2.0.4 (build 270014). All queries were limited to single crustal structures that contained 3D coordinates and had an R-factor of ≤ 0.1.

It appeared that the CSD contains 4.445 CIFs with an AuX_4 structure where X can be any atom and the Au–X bonds were set as 'any bond'. These CIFs were further inspected for instances where any electron rich atom (ElR = N, P, As, O, S, Se, Te, F, Cl, Br, I, At) has a maximum *inter*molecular Au···ElR distance (***d***) of 2 Å + the Bondi van der Waals radii of Au (1.66 Å) and ElR (see also the inset figure on the left-hand side of Figure 6). The four X–Au···ElR angles (α) were measured as well and the shortest was used in the analysis. This query resulted in 24.868 distance-angle pairs contained within 2.781 CIFs, which were binned and plotted as the heat plot shown in the left-hand side of Figure 6 (using Origin 2018). A plot of a similar dataset limited to ElR = any halogen atom is shown in Figure S4 (13.139 [***d'*** ; α] pairs within 1.654 CIFs).

A plot of a similar dataset limited to $[AuHlg_3N]$ complexes is shown in the left-hand side of Figure S5 (508 [***d'*** ; α] pairs within 86 CIFs). 93% of these data (i.e. 472 [***d'*** ; α] pairs in 77 CIFs) involve a $[AuCl_3N]$ complex and the accompanying heat plot is shown in the right-hand side of Figure S5. All the 77 CIFs used for Figure S5 (right) are listed in Table S4, together with the electron rich atom (ElR), the van der Waals corrected Au···ElR distance (***d'***) according to Bondi and Batsanov, and the smallest N/Cl–Au···ElR angle (α) that are associated with the shortest intermolecular Au···ElR distance measured for each CIF. In this table, the data characterized by van der Waals overlap has been highlighted in green, which is 14% using Bondi's van der Waals radius of Au (1.66 Å) and 43% using Batsanov's van der Waals radius of Au (1.86 Å).

A similar search revealed that the CSD contains a total of 1.556 CIFs with an X_3AuHlg complex where Hlg can be any halogen atom. Within these structures, 523 CIFs were identified where two X_3AuHlg complexes are characterized by two $d' \leq 2$Å intermolecular (Bondi) van der Waals corrected Au···Hlg distances (see also the inset figure on the right-hand side of Figure 6). Both Au–Hlg···Au angles (β) were measured as well, which resulted in 1.636 distance-angle [***d'*** ; β] pairs within 818 CIFs. The pairs with the shortest ***d'*** (and accompanying β) were used to generate the heat plot sown on the right-hand side of Figure 6 (i.e., using 818 [***d'*** ; β] pairs). Plotting all 1.636 [***d'*** ; β] pairs gave a nearly identical heat plot, as is shown in Figure S6.

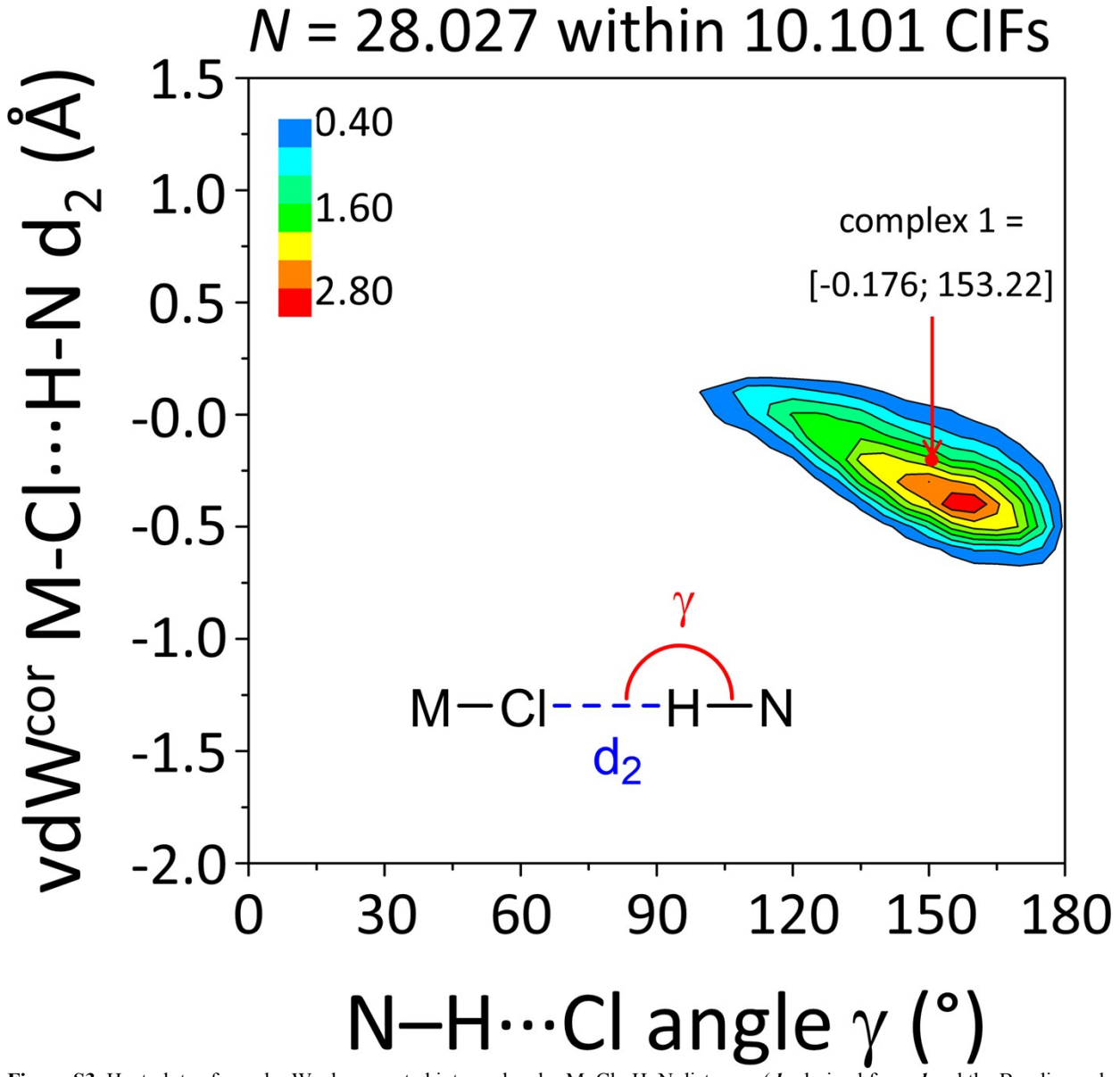

Figure S3. Heat plots of van der Waals corrected intermolecular M–Cl···H–N distances (d_2, derived from d and the Bondi van der Waals radii of Cl (1.75) and H (1.09)) as a function of N – H···Cl angle γ (see inset Figure). M can be any metal and the M–Cl bond was set to any bond. The 28.027 unique data points (N) are data are contained within 10.101 CIFs (searching only structures with 3D coordinates, an R-factor of 0.1 or below and excluding powder XRD structures. The geometric information of complex 1 is indicated in the figure and can be seen as moderate (in between the clear peak at [-0.5; 160] and the tail around [0; 120].

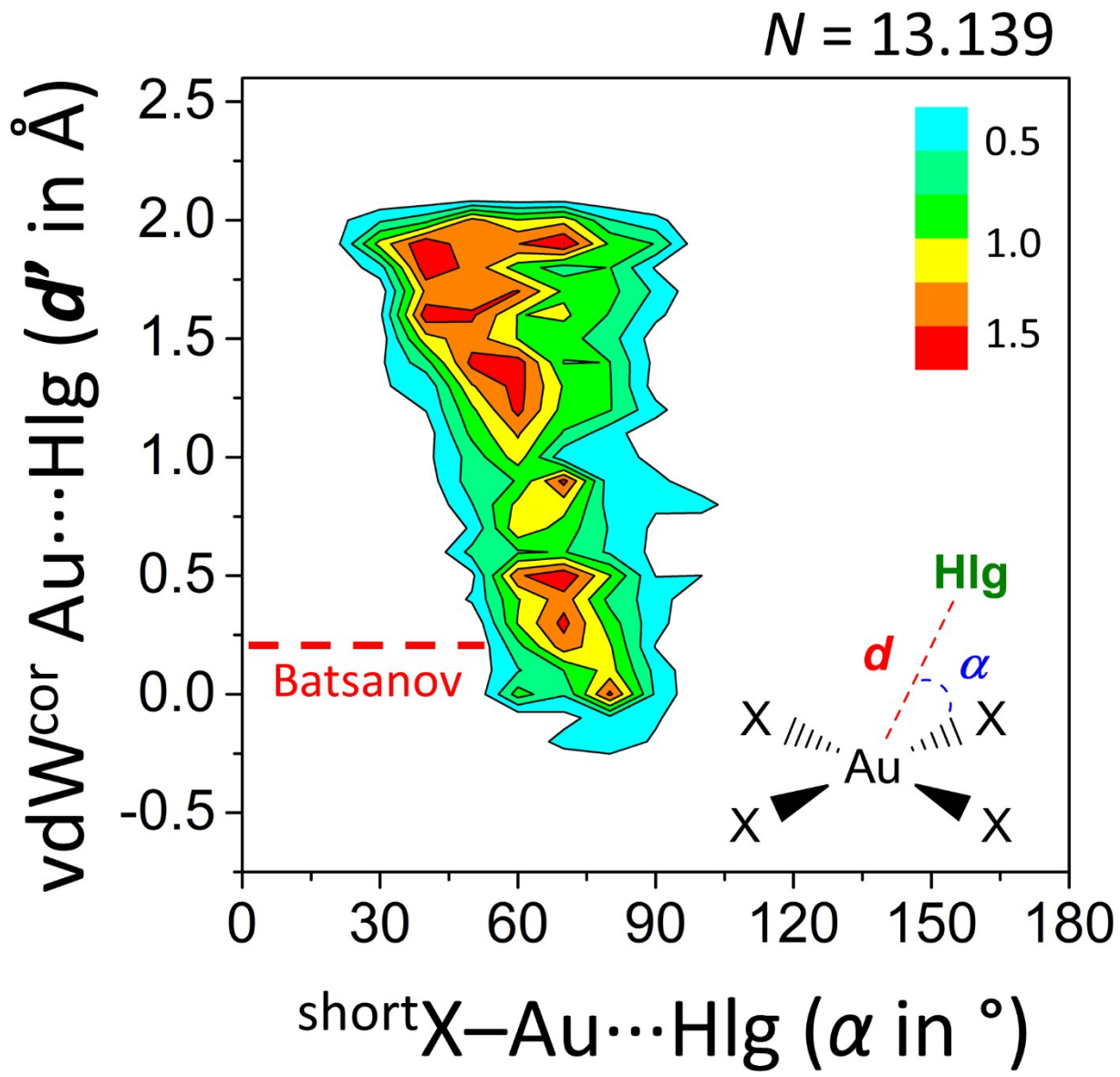

Figure S4. Heat plots of van der Waals corrected intermolecular Au···Y distances (***d'***, derived from ***d*** and the Bondi van der Waals radii of Au and Hlg) as a function of angle α (see inset Fig., the shortest angle was used). The plot involves 13.139 hits contained within 1.654 CIFs. Hlg = any halogen atom, X = any atom, and data involves Au···Y distances ***d'*** ≤ 2 Å). The red dashed line represents van der Waals overlap using Batsanov's van der Waals radius for Au (1.86 Å). See Figure 6 (left) for the plot of a similar dataset involving any electron rich atom instead of only halogens (ElR = N, P, As, O, S, Se, Te, F, Cl, Br, I, At).

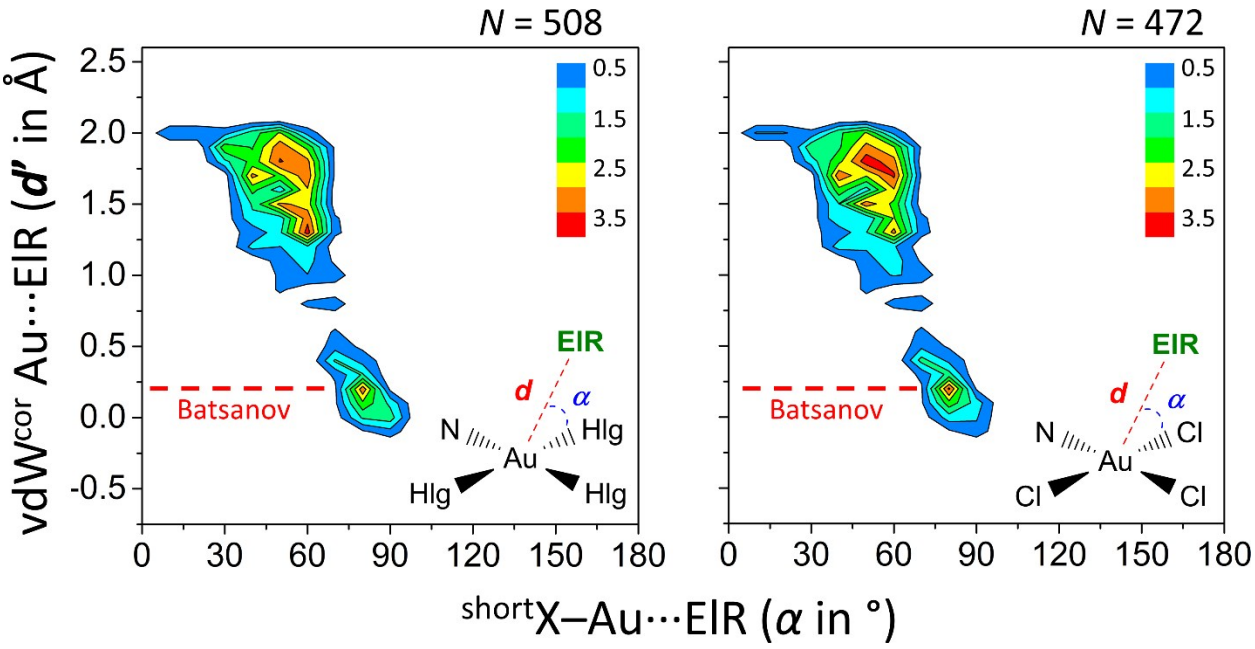

Figure S5. Heat plots of van der Waals corrected intermolecular Au···ElR distances (***d'***, derived from ***d*** and the Bondi van der Waals radii of Au and Hlg) as a function of angle α (see inset Fig.s, the shortest angle was used). Left: 508 hits contained within 86 CIFs involving [$AuHlg_3N$] complexes. Right: 4728 hits contained within 77 CIFs involving [$AuCl_3N$] complexes. ElR = N, P, As, O, S, Se, Te, F, Cl, Br, I, At; Hlg = any halogen atom; data involves Au···ElRY distances ***d'*** ≤ 2 Å. The red dashed line represents van der Waals overlap using Batsanov's van der Waals radius for Au (1.86 Å).

Table S4. Overview the 77 CIFs used for Figure S3 (right) together with relevant (geometric) data of the shortest intermolecular Au···ElR distance found for each CIF. Data characterized by van der Waals overlap has been highlighted in green.

		d′ **(shortest) in Å**						***d′*** **(shortest) in Å**		
CIF:	**ElR**	**Bondi**	**Batsanov**	**α (°)**	**CIF:**	**ElR**	**Bondi**	**Batsanov**	**α (°)**
WIRGAH	Cl	-0.124	-0.324	85.9	BUVVIY	Cl	0.248	0.048	84.6
RIMFIF	Cl	-0.097	-0.297	75.8	YIDMAA	Cl	0.249	0.049	85.0
SEVXID	Cl	-0.073	-0.273	80.9	ELUVAK	Cl	0.263	0.063	80.2
NOKMUX	Cl	-0.057	-0.257	87.8	VOYNUU	Cl	0.263	0.063	83.4
ZUHNIB	Cl	-0.054	-0.254	85.1	XIMWOI	Cl	0.281	0.081	79.7
VANPUY	Cl	-0.052	-0.252	85.4	KUFNAB	Cl	0.286	0.086	71.8
NOKMOR	Cl	-0.047	-0.247	86.7	SASRIQ	Cl	0.308	0.108	76.6
FEYTEI	Cl	-0.017	-0.217	80.7	EHEXOG	Cl	0.349	0.149	78.4
HAFFIE	Cl	-0.010	-0.210	73.2	MIYZAY	Cl	0.376	0.176	79.7
SASREM	Cl	-0.003	-0.203	87.4	HOSHII	Cl	0.377	0.177	85.5
BUWVUM	Cl	-0.002	-0.202	84.1	KOXQEV	Cl	0.406	0.206	73.8
SASREM01	Cl	0.005	-0.195	87.3	DEDYUG	Cl	0.436	0.236	80.4
KILFIV	Cl	0.015	-0.185	85.7	QIHVOS	Cl	0.445	0.245	72.2
HOSHUU	Cl	0.032	-0.168	84.5	DIWYIU	Cl	0.460	0.260	69.9
SOVROM	Cl	0.042	-0.158	80.7	HAFFEA	Cl	0.474	0.274	84.6
NOKNAE	Cl	0.050	-0.150	86.4	TIGMIH	S	0.499	0.299	65.9
EHEXIA	Cl	0.060	-0.140	85.6	BUVVAQ	Cl	0.609	0.409	85.2
ZUHNOH	Cl	0.064	-0.136	75.2	KOXQAR	Cl	0.798	0.598	65.9
BIRCUA	Cl	0.069	-0.131	79.4	SUYXER	N	0.914	0.714	62.0
AVATUN	Cl	0.070	-0.130	76.3	MUPHIP	N	0.951	0.751	58.2
GOXCAX	Cl	0.090	-0.110	86.7	BIXBOZ10	N	0.982	0.782	59.7
ZUHNAT	Cl	0.102	-0.098	74.7	TIRMEP	Cl	1.124	0.924	75.9
MOCFER	Cl	0.109	-0.091	82.4	CDMPAU01	Cl	1.221	1.021	40.5
WONZUX	Cl	0.114	-0.086	86.2	DODXID	Cl	1.251	1.051	30.4
MOCFUH	Cl	0.118	-0.082	81.0	CDMPAU	Cl	1.318	1.118	39.5
FEDTUF	Cl	0.129	-0.071	82.9	SUYXIV	Cl	1.326	1.126	81.2
UQIBEC	Cl	0.142	-0.058	87.8	CPYQAU	Cl	1.345	1.145	59.2
MAJDAC	Cl	0.153	-0.047	83.4	DIWXAL	Cl	1.350	1.150	41.3
DOYPOY	Cl	0.172	-0.028	80.7	DIWWUE	Cl	1.455	1.255	39.3
GOXCUR	Cl	0.184	-0.016	80.3	NIYTIA	Cl	1.662	1.462	47.5
VEGMEZ	Cl	0.185	-0.015	65.8	OJELIA	N	1.672	1.472	57.6
MIYYOL	Cl	0.193	-0.007	87.5	AUBQNL01	Cl	1.711	1.511	38.6
RADLAJ	Cl	0.200	0.000	76.3	VUFXIE	Cl	1.770	1.570	50.8
QAWDEA	Cl	0.220	0.020	76.8	ZUHNUN	Cl	1.903	1.703	42.2
VOYPAC	Cl	0.220	0.020	85.2	HORVIV	N	1.953	1.753	22.5
PYAUCL10	Cl	0.226	0.026	79.5	LUVRIF	Cl	1.955	1.755	47.3
MIYZEC	Cl	0.230	0.030	82.4	AZTLAW	N	1.957	1.757	40.6
SUYXAN	Cl	0.230	0.030	68.6	LAYPUY	Cl	1.969	1.769	61.2
HIHCIK	Cl	0.246	0.046	82.3					

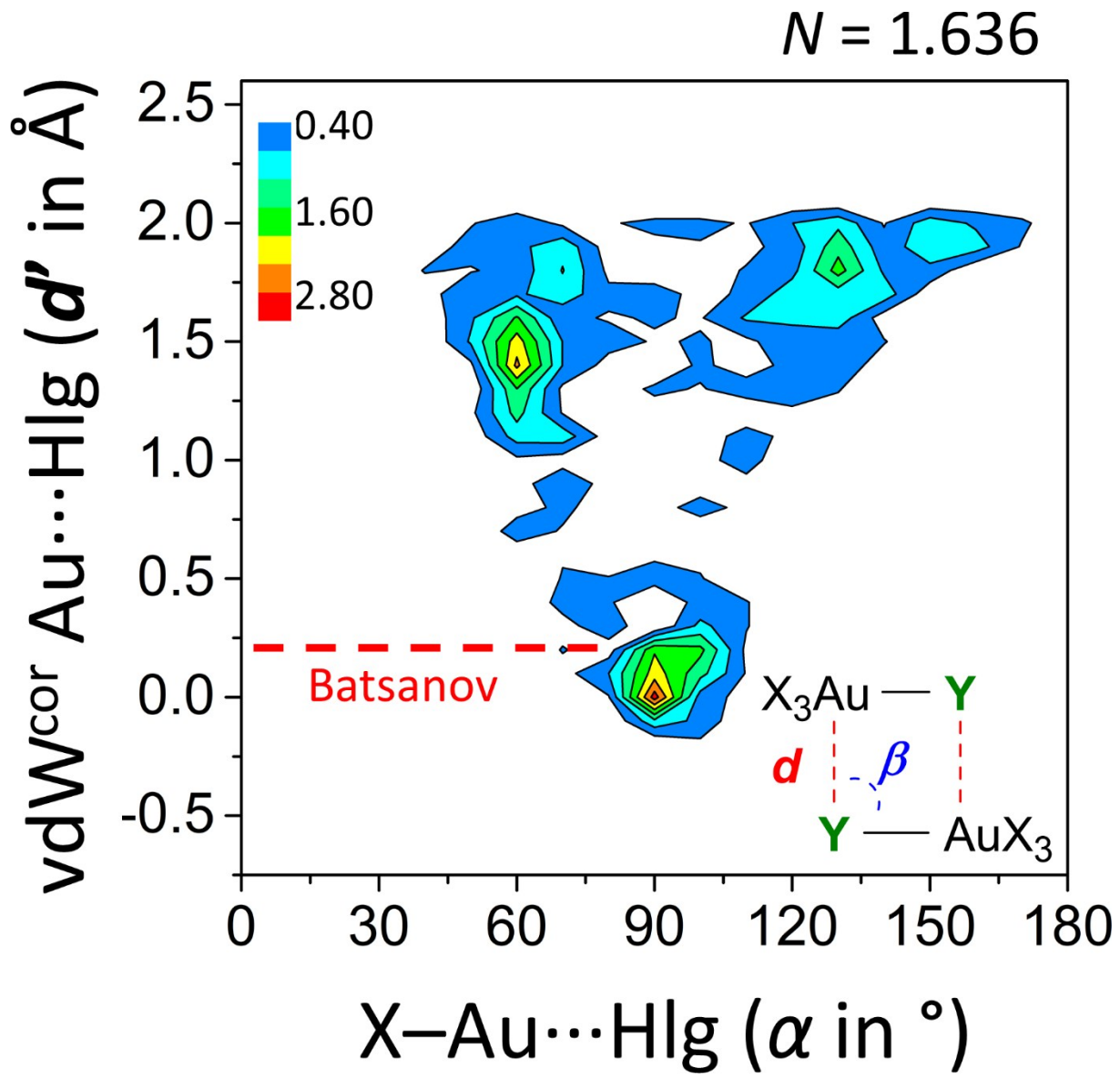

Figure S6. Heat plots of van der Waals corrected intermolecular Au···Hlg distances (***d'***, derived from ***d*** and the Bondi van der Waals radii of Au and Hlg) as a function of X–Au···Hlg angle β. Both distance-angle pairs (1.636 within 532 CIFs) of the dimer (see inset Fig.) were used to generate this plot, as opposed to only the shortest distance (and related angle) used in Fig. 6. Hlg = any halogen (F, Cl, Br, I, At), X can be any atom and the queries (illustrated in the inset Figuress) involved data with Au···Y distances ***d*** of ≤ the Bondi van der Waals radii of Au and Hlg + 2 Å. The red dashed line represents van der Waals overlap using Batsanov's van der Waals radius for Au (1.86 Å).

References:

[1] M. Barceló-Oliver, B. A. Baquero, A. Bauzá, A. García-Raso, A. Terrón, I. Mata, E. Molins, A. Frontera, CrysEngComm **2012**, *14*, 5777–5784.
[2] SADABS, Bruker-AXS, Version 1, Bruker AXS Inc., Madison, WI, **2004**.
[3] L.J. Farrugia, WinGX suite for small-molecule single-crystal crystallography. *J. Appl. Crystallogr.* **1999**, *32*, 837–838.
[4] G.M. Sheldrick, Crystal structure refinament with SHELXL. *Acta Crystallogr.* **2015**, *C71*, 3–8.
[5] G.M. Sheldrick, SHELXL-2017/1, Program for the Solution of Crystal Structures, University of Göttingen, Germany, **2017**.
[6] A.L. Spek, *Acta Crystallogr.* **2009**, *D65*, 148–155.
[7] Gaussian 16, Revision C.01, M. J. Frisch, G. W. Trucks, H. B. Schlegel, G. E. Scuseria, M. A. Robb, J. R. Cheeseman, G. Scalmani, V. Barone, G. A. Petersson, H. Nakatsuji, X. Li, M. Caricato, A. V. Marenich, J. Bloino, B. G. Janesko, R. Gomperts, B. Mennucci, H. P. Hratchian, J. V. Ortiz, A. F. Izmaylov, J. L. Sonnenberg, D. Williams-Young, F. Ding, F. Lipparini, F. Egidi, J. Goings, B. Peng, A. Petrone, T. Henderson, D. Ranasinghe, V. G. Zakrzewski, J. Gao, N. Rega, G. Zheng, W. Liang, M. Hada, M. Ehara, K. Toyota, R. Fukuda, J. Hasegawa, M. Ishida, T. Nakajima, Y. Honda, O. Kitao, H. Nakai, T. Vreven, K. Throssell, J. A. Montgomery, Jr., J. E. Peralta, F. Ogliaro, M. J. Bearpark, J. J. Heyd, E. N. Brothers, K. N. Kudin, V. N. Staroverov, T. A. Keith, R. Kobayashi, J. Normand, K. Raghavachari, A. P. Rendell, J. C. Burant, S. S. Iyengar, J. Tomasi, M. Cossi, J. M. Millam, M. Klene, C. Adamo, R. Cammi, J. W. Ochterski, R. L. Martin, K. Morokuma, O. Farkas, J. B. Foresman, and D. J. Fox, Gaussian, Inc., Wallingford CT, 2016.
[8] F. Weigend, *Phys. Chem. Chem. Phys.* **2006**, *8*, 1057–1065.
[9] F. Weigend, R. Ahlrichs, *Phys. Chem. Chem. Phys.* **2005**, *7*, 3297–3305.
[10] C. Adamo, V. Barone, *J. Chem. Phys*., **1999**, *110*, 6158-6169.
[11] R. F. W. Bader, M. T. Carroll, J. R. Cheeseman, C. Chang, *J. Am. Chem. Soc*. **1987**, *109*, 7968–7979.
[12] R. F. W. Bader, Atoms in Molecules, A Quantum Theory, Clarendon, Oxford, **1990**.
[13] AIMAll (Version 17.11.14), T. A. Keith, TK Gristmill Software, Overland Park KS, USA, (aim.tkgristmill.com), 2013